Journal of Solid State Chemistry 181 (2008) 2227–2230

Contents lists available at ScienceDirect

Journal of Solid State Chemistry

journal homepage: www.elsevier.com/locate/jssc

The role of orbital ordering in the tetragonal-to-cubic phase transition in $CuCr_2O_4$

Brendan J. Kennedy *, Qingdi Zhou

The School of Chemistry, The University of Sydney, Sydney NSW 2006, Australia

ARTICLE INFO

Article history:
Received 29 February 2008
Received in revised form
29 April 2008
Accepted 1 May 2008
Available online 20 May 2008

Keywords:
Orbital order
Jahn–Teller distortion
Phase transition
Spinel

ABSTRACT

Copper(II) chromite ($CuCr_2O_4$) undergoes a first-order structural transition from a tetragonal distorted spinel structure in space group ($I4_1/amd$) to a cubic spinel structure in $Fd\bar{3}m$, near 600 °C. The transition has been followed using synchrotron X-ray powder diffraction between room temperature and 750 °C. The structure changes as a consequence of a transition from an orbitally ordered to orbital disordered state associated with a Jahn–Teller-type distortion of the CuO_4 tetrahedron. The orbital melting results in a small increase in cell volume.

1. Introduction

Copper(II) chromite ($CuCr_2O_4$) is a tetragonally distorted spinel with $c/a<1$ [1,2]. This distortion from the archetypical cubic spinel structure is a consequence of the Jahn–Teller effect in the Cu^{2+} cation. The Cu^{2+} cations occupy the four-coordinate sites of the spinel structure, and removal of the degeneracy of the d^9 ground state results in flatting of the CuO_4 tetrahedron lowering the symmetry to tetragonal. The structure of $CuCr_2O_4$ transforms to that of a cubic spinel near 600 °C, at which point the compression of the CuO_4 tetrahedron is removed [3,4]. $CuCr_2O_4$ is a versatile catalyst finding application in a range of applications including CO oxidation and alcohol dehydrogenation [5]. Most of these processes operate at temperatures near the tetragonal–cubic transition point. Cr spinels are also of interest in the earth sciences, with spinels being stable over a wide range of temperatures and pressures [6]. Recently there has been considerable interest in the structural transitions in chromite spinels, and in particular for $NiCr_2O_4$ [7–11]. As reported for $CuCr_2O_4$, $NiCr_2O_4$ exhibits a phase transition from the cubic spinel structure to a tetragonal variant, albeit at lower temperatures, near 30 °C as a result of the Jahn–Teller effect. $MgCr_2O_4$ is also reported to become tetragonal upon cooling below 15 K [12]. In contrast with the detailed structural studies of $NiCr_2O_4$, very little is known regarding the cubic–tetragonal structural transition in $CuCr_2O_4$, although the elastic properties associated with this transition continue to gain interest [13].

In this paper we present the results of a high-resolution synchrotron X-ray powder diffraction study of the tetragonal–cubic phase transition in $CuCr_2O_4$. We show that this process is first order and involves a transition from an orbitally ordered structure to an orbitally disordered one. The loss, or melting, of this orbital order results in a small discontinuous increase in the cell volume.

2. Experimental

A crystalline sample of $CuCr_2O_4$ was prepared by the reaction of stoichiometric quantities of $Cu(NO_3)_2 \cdot 2.5H_2O$ (99.8% Univar) and Cr_2O_3 (99.9%, Aldrich). A concentrated solution of $Cu(NO_3)_2$ was mixed with solid Cr_2O_3 and the resulting slurry was stirred and evaporated to dryness. The resulting solid was then heated in an alumina crucible at 700 °C for 16 h. After re-grinding the material was formed into a 13 mm diameter pellet and calcined at 900 °C for 48 h, slowly cooled to 700 °C and sintered at this temperature for 66 h before being cooled to room temperature. Preliminary X-ray powder patterns recorded using Cu $K\alpha$ radiation indicated the formation of a single-phase sample.

Synchrotron X-ray diffraction data were collected on the Debye Scherrer diffractometer at the Australian National Beamline Facility, Beamline 20B at the Photon Factory, Tsukuba, Japan [14]. The sample was housed in an open-ended 0.3 mm diameter capillary that was rotated during the measurements. Data at room temperature were recorded in the angular range $5<2\theta<85°$, step

---

* Corresponding author. Fax: +61 2 9351 3329.
E-mail address: B.Kennedy@chem.usyd.edu.au (B.J. Kennedy).

0022-4596/$ - see front matter Crown Copyright © 2008 Published by Elsevier Inc. All rights reserved.
doi:10.1016/j.jssc.2008.05.018

size 0.01° using X-rays of wavelength 0.80155 Å. Variable temperature data were collected, using a custom-built furnace, at temperatures of up to 750 °C. The structures were refined using the program RIETICA [15]. It should be noted that a small amount of decomposition of the sample was observed at temperatures above 650 °C. We ascribe this to partial reduction of the spinel under the vacuum conditions of the diffractometer. We believe that this does not impact on the conclusions of this work.

3. Results and discussion

The diffraction pattern of $CuCr_2O_4$ at room temperature could be indexed to a body-centered tetragonal structure with $a_{tet} \sim a_{cub}/\sqrt{2} = 6.03$ Å and $c_{tet} \sim c_{cub} = 7.81$ Å (Fig. 1).

The structure was refined in space group ($I4_1/amd$) with the Cu on the 4*a* site, Cr on 8*d* and O on the 16*h* site, as proposed by Dollase and ONeill. The refined structural parameters are summarized in Table 1, and these are in good agreement with the results described by Dollase and ONeill [2]. The unique Cu–O distance is 1.983(2) Å and the Cu bond valence sum (1.76) is slightly lower than expected but consistent with divalent Cu. The CrO_6 is slightly elongated with two longer (1.990(3) Å) and four shorter (1.972(2) Å) Cr–O distances with the average Cr–O distance being 1.978 Å and the effective bond valence sum being 3.02. The compression of the CuO_4 tetrahedron results in two O–Cu–O angles of 123.2(2)° and 103.1(1)°, respectively.

Heating the sample results in a gradual increase in the *c*-lattice parameters, whereas the *a* parameter remains approximately constant near 500 °C at which point it decreases some what. Above 600 °C, the tetragonal splitting is abruptly lost and the pattern could be indexed to a face-centered cubic cell with $a_{cub} \sim 8.35$ Å. The structural parameters for the sample at 750 °C obtained by refining the cubic structure in space group $Fd\bar{3}m$ are also listed in Table 1. At this temperature both the Cu–O (1.993(5) Å) and Cr–O (1.988(3) Å) distances are slightly longer than their room temperature equivalents. The O–Cu–O angle is, by symmetry requirements, 109.4° in the cubic structure (Fig. 2).

The temperature dependence of the angles within the CuO_4 tetrahedron is illustrated in Fig. 3. The JT-induced distortion of the CuO_4 tetrahedron results in four O–Cu–O angles that are smaller than the ideal tetrahedron angle of 109.4° and two larger angles. These angles reflect the compression of the CuO_4 tetrahedron. Heating results in a gradual reduction in the compression of the

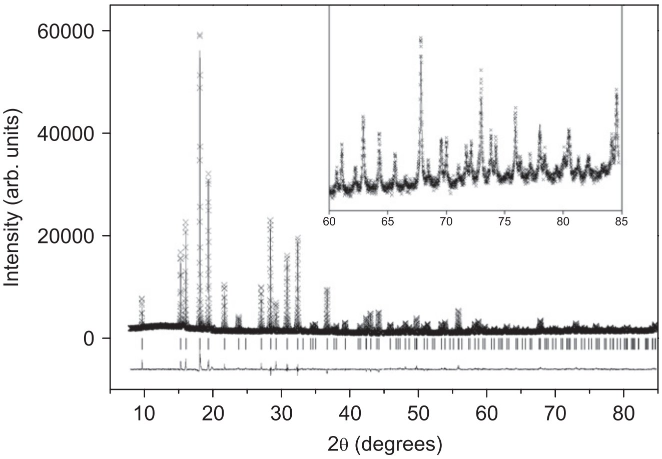

Fig. 1. Observed calculated and difference synchrotron X-ray diffraction profiles for $CuCr_2O_4$ at room temperature. The data were collected with $\lambda = 0.80155$ Å. The inset highlights the quality of the data to high angles.

Table 1
Lattice parameters and atomic positions of tetragonal and cubic structures of $CuCr_2O_4$

Space group	$I4_1/amd$	$Fd\bar{3}m$
Temperature (°C)	25	750
a (Å)	6.0316(1)	8.3543(3)
c (Å)	7.7837(2)	= *a*
Cu	4*a* (0,1/4,1/8)	8*a* (1/8,1/8,1/8)
B ($Å^2$)	1.48(3)	2.88(7)
Cr	8*d* (0,0,0)	16*d* (0,0,0)
B ($Å^2$)	0.59(3)	1.47(5)
O	16*h* (0,*y*,*z*)	32*e* (*x*,*x*,*x*)
	$y = 0.5344(4)$	$x = 0.2627(4)$
	$z = 0.2555(4)$	
B ($Å^2$)	1.37(7)	3.01(12)
R_p (%)	4.55	5.44
R_{wp} (%)	5.86	6.99

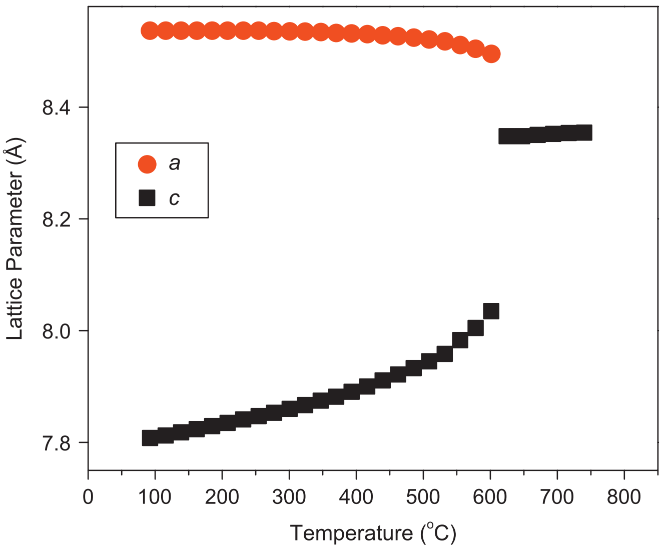

Fig. 2. Temperature dependence of the lattice parameters for $CuCr_2O_4$ obtained from Rietveld refinements of synchrotron X-ray powder diffraction data. For ease of comparison the *a* parameters in the low-temperature tetragonal phase have been multiplied by $\sqrt{2}$.

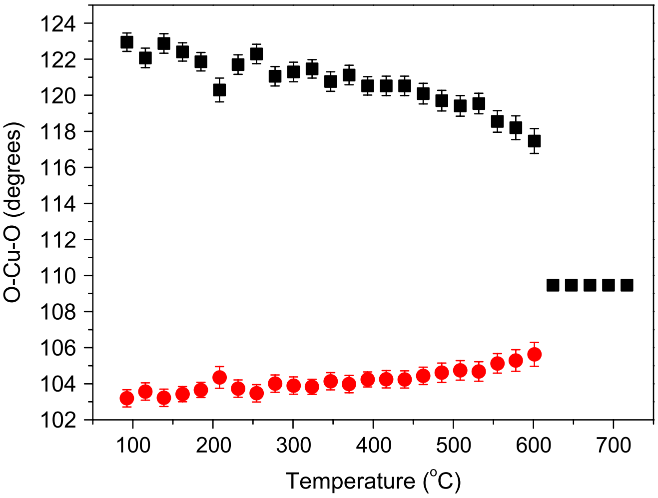

Fig. 3. Temperature dependence of the angles within the CuO_4 tetrahedra.

CuO_4 tetrahedron but clearly the compression remains significant until near the transition temperature, at which point the distortion of the tetrahedral rapidly vanishes. The abrupt change in the O–Cu–O angles mimics the change in the lattice parameters, and it appears from either measure that the transition to cubic is first order. $CuRh_2O_4$ also displays a first-order tetragonal-to-cubic transition associated with the removal of a Jahn–Teller-induced distortion [16].

One method by which the transition can be monitored is by examination of the temperature dependence of the spontaneous tetragonal strains defined by $\varepsilon_t = ((a_{tet} - c_{tet})/(a_{tet} + c_{tet}))$. The transition between the tetragonal and cubic states can be described by an order parameter Q. According to the Landau theory [17] for a second-order ferroelastic transition the spontaneous strain ε_s is expected to be closely proportional to the lowest-order term to which it couples, namely Q^2 [18,19].

For a second-order phase transition Q^2 is expected to be proportional to T, and as is evident from Fig. 4 this is clearly not observed. Rather analysis suggests an unrealistic Q^6 temperature dependence. Moreover at the critical temperature the strain drops much more rapidly than, even this complex, relationship predicts. The group–subgroup relationship of the two space groups allows for a continuous transition but does not require it. Apparently the tetragonal structure gradually evolves towards the archetypal cubic one upon heating, but the final stages of the transition occurs abruptly. This first-order quenching of the Jahn–Teller distortion is similar to that observed for $LaMnO_3$ [20], where again the transition appears to be continuous until very close to transition temperature.

Fig. 5 shows the temperature dependence of the, suitably scaled between the two space groups, unit cell volume of $CuCr_2O_4$. The volume progressively increases up to 600 °C, at which point it jumps abruptly. This volume anomaly is similar to that seen in $LaMnO_3$, but is of the opposite sense; in $LaMnO_3$ the volume decreases at the Jahn–Teller transition [21]. Chatterji and co-workers [21] have suggested that the volume decrease in $LaMnO_3$ arises since the Jahn–Teller distortion induces orbital ordering with the Jahn–Teller distorted octahedra occupying more volume. Removal, or melting, of this orbital ordering results in a contraction in the volume of the MnO_6 octahedra and subsequently in the unit cell. It must be stressed that, although attracting considerable attention, the volume contraction upon orbital melting in $LaMnO_3$ is, like the volume contraction at the melting point of ice, an anomaly, For the vast majority of materials, increased entropy of the disordered structure results in an increase in volume in the liquid state compared with the solid state. For $CuCr_2O_4$ orbital melting results in an increase in volume as expected for a simple material.

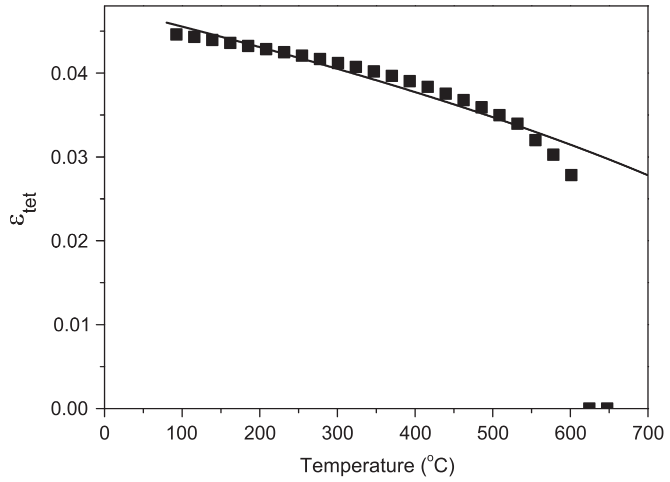

Fig. 4. Temperature dependence of the tetragonal strain in $CuCr_2O_4$. The solid line shows the behavior expected for a second-order phase transition.

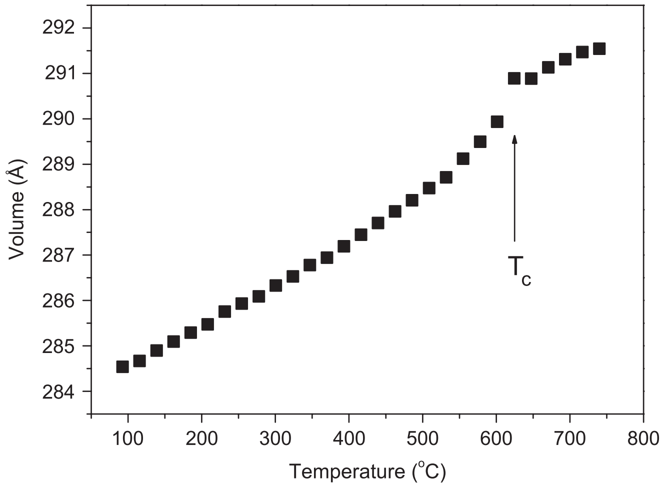

Fig. 5. Temperature dependence of volume of $CuCr_2O_4$.

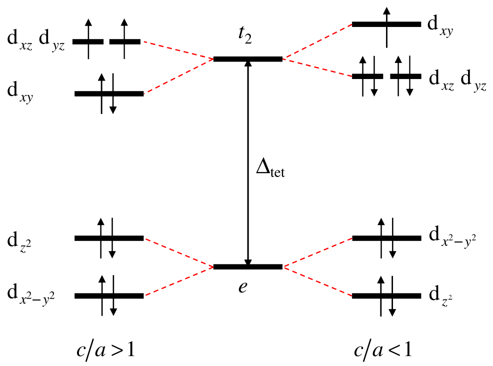

Fig. 6. Schematic d orbital energy diagram for a d^8 (Ni^{2+}) in a elongated tetrahedron with $c/a>1$ and a d^9 (Cu^{2+}) ion in a compressed tetrahedron with $c/a<1$. Note that in the Ni case the ground state is doubly degenerate and hence susceptible to further distortion.

Finally it is pertinent to compare our results with those reported for $NiCr_2O_4$. The higher transition temperature observed for $CuCr_2O_4$~600 °C cf $NiCr_2O_4$~30 °C demonstrates the energy required to overcome the Jahn–Teller-type distortion of the $Cu^{II}O_4$ tetrahedron is considerably greater than that for the $Ni^{II}O_4$ tetrahedron. Ligand field arguments [22–24] suggest that the JT effect will lead to a larger distortion in the Cu^{2+} case than that in the Ni^{2+} case and that the distortion of the tetrahedron will be of an opposite sense, since in the d^9 Cu^{2+} the doubly degenerate d_{xz} and d_{yz} orbitals will both be fully occupied, whereas in d^8 Ni^{2+} these will be singly occupied (see Fig. 6). Equally importantly a single distortive mode (to the tetragonal structure) results in a double degenerate ground state for the Ni^{2+} complex, without any appreciable energy gain. It may be anticipated, therefore, that this will undergo a further distortion. The observed [4] behavior of $CuCr_2O_4$ and $NiCr_2O_4$ support these arguments, with the transition to the tetragonal occurring at much lower temperatures in the Ni oxide, and this tetragonal phase exists over a narrow temperature range, before a second transition to an orthorhombic structure that will have a singularly degenerate ground state as required by the Jahn–Teller theorem. It appears from the work of Tovar and co-workers [4] that the $I4_1/amd$ to $Fd\bar{3}m$ transition in $NiCr_2O_4$ is also first order. $MgCr_2O_4$ also displays at tetragonal

($I4_1/amd$)–cubic ($Fd\bar{3}m$) transition, albeit at still lower temperatures, below 15 K [12]. In this case the transition is clearly not driven by the Jahn–Teller effect of the spinal A-type cation but rather appears to be driven by a distortion of the CrO_6 octahedron that may be correlated with magnetic ordering. It would be interesting to establish if, in this case, the transition is continuous as allowed by group theory.

Acknowledgments

This work has been partially supported by the Australian Research Council. The work performed at the Australian National Beamline Facility was supported by the Australian Synchrotron Research Program, which is funded by the Commonwealth of Australia under the Major National Research Facilities program. We thank Dr. Garry Foran for assistance at the ANBF.

References

[1] Z.-G. Yé, O. Crottaz, F. Vaudano, F. Kubel, P. Tissot, H. Schmid, Ferroelectrics 162 (1994) 103–118.
[2] W.A. Dollase, H.S. ONeill, Acta Crystallogr. C-Cryst. Struct. Commun. 53 (1997) 657–659.
[3] K.S. De, J. Ghose, K.S.R.C. Murthy, J. Therm. Anal. 22 (1981) 13–16.
[4] M. Tovar, R. Torabi, C. Welker, F. Fleischer, Phys. B: Condens. Matter 385–386 (2006) 196–198.
[5] L.M. Plyasova, I.Y. Molina, T.A. Kriger, L.P. Davydova, V.V. Malakhov, L.S. Dovlitova, T.M. Yur'eva, Kinet. Catal. 42 (2001) 126–131.
[6] S. Klemme, Lithos 77 (2004) 639–646.
[7] E. Prince, Acta Crystallogr. 10 (1957) 554–556.
[8] H. Ishibashi, T. Yasumi, J. Magn. Magn. Mater. 310 (2007) E610–E612.
[9] T. Armbruster, G.A. Lager, J. Ihringer, F.J. Rotella, J.D. Jorgensen, Z. Kristallogr. 162 (1983) 8–10.
[10] G. Ueno, S. Sato, Y. Kino, Acta Crystallogr. C-Cryst. Struct. Commun. 55 (1999) 1963–1966.
[11] Y. Kino, B. Lüthi, M.E. Mullen, J. Phys. Soc. Japan 33 (1972) 687–697.
[12] H. Ehrenberg, M. Knapp, C. Baehtz, S. Klemme, Powder Diffr. 17 (2002) 230–233.
[13] V.V. Ivanov, V.M. Talanov, N.P. Shaberskaya, Inorg. Mater. 36 (2000) 1167–1172.
[14] T.M. Sabine, B.J. Kennedy, R.F. Garrett, G.J. Foran, D.J. Cookson, J. Appl. Crystallogr. 28 (1995) 513–517.
[15] C.J. Howard, B.A. Hunter, A Computer Program for Rietveld Analysis of X-ray and Neutron Powder Diffraction Patterns, Lucas Heights Research Laboratories, NSW, Australia, 1998, pp. 1–27.
[16] I. Ismunandar, B.J. Kennedy, B.A. Hunter, Mater. Res. Bull. 34 (1999) 135–143.
[17] M.A. Carpenter, Am. Mineral. 92 (2007) 309–327.
[18] D. Errandonea, EPL 77 (2007) 56001.
[19] L.D. Landau, E.M. Lifshitz, Statistical Physics Part 1, in Course of Theoretical Physics, vol. 5, third ed., Pergamon Press, Oxford, 1994.
[20] J. Rodrıguez-Carvajal, M. Hennion, F. Moussa, A.H. Moudden, L. Pinsard, A. Revcolevschi, Phys. Rev. B 57 (1998) R3189–R3192.
[21] T. Chatterji, F. Fauth, B. Ouladdiaf, P. Mandal, B. Ghosh, Phys. Rev. B 68 (2003) 052406.
[22] J.D. Dunitz, E. Orgel, J. Phys. Chem. Solids 3 (1957) 20–29.
[23] D. Reinen, M. Atanasov, G. Stnikolov, F. Steffens, Inorg. Chem. 27 (1988) 1678–1686.
[24] L.E. Nestour, A. Gaudon, M. Villeneuve, G. Andriessen, A. Demourgues, Inorg. Chem. 46 (2007) 2645–2658.